POLITECNICO
MILANO 1863

SCUOLA DI INGEGNERIA INDUSTRIALE
E DELL'INFORMAZIONE

Synthesis and structural characterization of metal organic cages (MOCs) using *exo*-tridentate *tris*-pyridyl ligands

TESI DI LAUREA MAGISTRALE IN
CHEMICAL ENGINEERING
INGEGNERIA CHIMICA

Author: **SIJIE MA**

Student ID: 939505
Advisor: Prof. Javier Martí-Rujas
Co-advisor: Stefano Elli
Academic Year: 2022-23

Abstract

Metal-organic cages (MOC_S) represent a class of metal-organic materials with well-defined structures, cavities, and engineered pores. They are coordination-driven self-assembly discrete structures comprising metal ions and organic ligands formed in both solvent and solid states. With these properties, MOC_S are good candidates to study host-guest binding properties, molecular separations, catalysis, gas adsorption, etc. Poly-[*n*]-catenanes can be defined as a set of mechanically interlocked molecules (MIM_S). In our case, the subset of poly-[*n*]-catenanes are polycatenanes formed of interlocked $M_{12}L_8$ nanocages, where the cages are formed by coordination the tridentate organic ligand (TPB/TPP) which is an aromatic ligand consists of three pyridine rings and one benzene/pyridine ring locates in the center and forms a tridentate shape and Zn(II) metal salts. Templating aromatic solvents plays a crucial role in the formation of the $M_{12}L_8$ poly-[*n*]-catenanes due to the π-π interaction between the aromatic parts of the host and the guest molecules.

Enlightened by Fujita's work, the incorporation of 90° coordination angles using -ethylenediamine palladium nitrate end-capping group, a square planar into metal–organic complex, using the *cis*-protection, the coordination nature of metal ion changes from divergent to convergent, thus, discrete (0D) structures can be generated efficiently without formation of any oligomeric or polymeric products. We designed to build an octahedron M_6L_4 cage via molecular paneling, using a tridentate shape panel TPB (tris-pyridyl benzene) in combination with ethylenediamine palladium nitrate. The cage formed in the solid state as observed by ^{1}H NMR, which means a solvent-free reaction.

The poly-[*n*]-catenanes of $M_{12}L_8$ with formula $[(ZnX_2)_{12}(TPB)_8]$, $[(ZnX_2)_{12}(TPP)_8]$, were synthesized from TPB/TPP and metal salts both by grinding and fast/slow

crystallization. The powder products obtained by grinding are amorphous phases that become crystalline after guest inclusion by using templating solvents such as methanol, dichlorobenzene, and chloroform. The products were characterized by X-ray crystallography, IR, thermogravimetric, and elemental analysis. Meanwhile, some experiments like molecule storage and gas exchange were successfully carried out to explore some functional properties of those materials.

Keywords: metal-organic cages (MOC_S); poly-[*n*]-catananes; molecular paneling; solvent-free; self-assembly.

Abstract in italiano

Le gabbie metallo-organiche (MOC_S) rappresentano una classe di materiali metallo-organici con strutture, cavità e pori ingegnerizzati ben definiti. Sono strutture discrete autoassemblanti guidate dal coordinamento che comprendono ioni metallici e leganti organici formati sia allo stato solvente che solido. Con queste proprietà, i MOC_S sono dotati della capacità di legame ospite-ospite, separazioni molecolari, catalisi di massa, ecc. I poly-[*n*]-catenani possono essere definiti come un insieme di molecole meccanicamente interconnesse (MIM_S). Nel nostro caso, il sottoinsieme dei poly-[*n*]-catenani è la nanogabbia $M_{12}L_8$, che è formata da un legame di coordinazione tra il legante organico tridentato e i sali metallici. Pertanto, l'architettura dei poly-[*n*]-catenani può essere prevista in base alla struttura della corrispondente gabbia $M_{12}L_8$. I solventi aromatici svolgono un ruolo cruciale nella formazione di poly-[*n*]-catenani a causa dell'interazione π-π tra le due parti aromatiche dell'ospite e dell'ospite.

Illuminato dal lavoro di Fujita, l'incorporazione di angoli di coordinazione di 90 ° di metalli di transizione - (etilendiammina) nitrato di palladio, un quadrato planare in strutture metallo-organiche, utilizzando la protezione cis, la natura di coordinazione del cambiamento di ioni metallici cambia da divergente a convergente, quindi, strutture discrete (0D) generano in modo efficiente senza formazione di alcun prodotto oligomerico. Abbiamo progettato di costruire una gabbia di ottaedro tramite pannelli molecolari, utilizzando un pannello di forma tridentata utilizzando TPB (tris-piridil benzene) in combinazione con nitrato di palladio (etilendiammina). La gabbia si è formata anche allo stato solido come osservato dagli spettri ^{1}H NMR, il che significa una reazione priva di solventi.

I poly-[*n*]-catenani di $M_{12}L_8$ sono $[(ZnX_2)_{12}(TPB)_8]$, $[(ZnX_2)_{12}(TPB)_8]$, sono stati in

grado di essere sintetizzati da TPB/TPP e sali metallici sia mediante macinazione che cristallizzazione veloce/lenta. La fattibilità del trasferimento della polvere ottenuta dalla macinazione dalla fase amorfa a quella cristallina è stata dimostrata utilizzando solventi templanti come metanolo, diclorobenzene e cloroformio. Il prodotto è stato caratterizzato da cristallografia a raggi X, IR, analisi termogravimetrica ed elementare. Nel frattempo, alcuni esperimenti come lo stoccaggio di molecole e lo scambio di gas sono stati condotti con successo per esplorare la funzione di questo materiale.

Parole chiave: gabbie metallo-organiche (MOC_S); poly-[*n*]-catanani; pannelli molecolari; senza solventi; autoassemblaggio.

CONTENT

Abstract ..... **II**

Abstract in italiano ..... **IV**

1 Introduction **1**

1.1 Metal-Organic Frameworks 1

1.1.1 Definition and Geometry 1

1.1.2 Synthesis method 3

1.2 Poly-[*n*]-catenanes 5

1.2.1 Structure of catenanes 5

1.2.2 Synthesis method of catenane 6

1.2.3 A case study of $M_{12}L_8$ poly-[*n*]-catenanes 9

1.3 0-Dimensional Metal-Organic Cages 11

1.3.1 square planar and organic ligands 11

1.3.2 Structure rises from 1-D to 3-D 12

2 Results and discussion **14**

2.1 Poly-[*n*]-catenane of $M_{12}L_8$ (TPP and Zinchalides) 14

2.1.1 A case study of one-dimensional poly-[*n*]-catenanes (TPPand $ZnCl_2$) [27] 14

2.1.2 Instant synthesis of TPP and zinc halides 15

2.1.3 Solid-state reaction and transformation from the amorphousphase to the crystalline phase 18

2.2 Zero-dimensional (0D) metal-organic cages(MOC) 21

2.2.1 Synthesis of square planar complex 21

2.2.2 A coordination square self-assembled from 4,4'-bipyridine and enPd$(NO_3)_2$ 23

2.2.3 Solid state synthesis of TPB and enPd$(NO_3)_2$ 25

3 Materials and research methods **30**

3.1 Analytical instruments 30

3.2 General procedures 31

3.2.1 Slow crystallization: three layers synthesis of TPB and zincsalts 31

3.2.2 Slow crystallization: three layers synthesis of 4,4'-bipyridine and enPd$(NO_3)_2$ 32

3.2.3 Fast crystallization of TPP and ZnX_2 (X=I, Br, Cl) 32
3.2.4 Neat grinding of TPP and ZnX_2 (X=I, Br, Cl) 32
3.2.5 Synthesis of $enPd(NO_3)_2$ 33
3.2.6 Neat grinding of $enPd(NO_3)_2$ and TPB at different timegradient 33
4 Conclusions and further studies 34
Bibliography 36
List of Figures 41
Ringraziamenti **..... 43**

1 Introduction

1.1 Metal-Organic Frameworks

1.1.1 Definition and Geometry

The history of porous materials starts with Zeolites, the primary examples of inorganic porous materials composed of silica, aluminum, sodium, etc. [1] The general pore size is less than 2 mm, and they can separate different gas molecules and catalyze organic molecules depending on their pore dimensions and chemistry. Unfortunately, due to the limited number of both natural or synthesized Zeolites, the chemical functionalization and structure control of this class of porous materials has been challenging. [2]

Metal-organic frameworks (MOFs), also known as porous coordination polymers (PCPs), are formed of metal ions and organic bridging ligands, and are considered post-zeolitic materials. The metal ions can be considered as primary building units (PBUs) which can be single metal ions or forming nodes that bind the arms of the organic linkers together to form a repeating structure. Metal-oxygen-carbon clusters, instead of metal ions alone, can be classified as secondary building units (SBUs).[3] MOFs with stable pore structures were first synthesized by Yaghi and Kitagawa research groups in1990, although PCPs were earlier characterized by Robson and coworkers in 1989.[4] [5]Due to properties such as large porosity, specific internal surface area, and adjustable pore size, functional MOF materials continue to emerge and are widely used in gas adsorption and separation, hazard gas purification, bulk catalysis, and drug delivery. A typical solution self-assembling process of a MOF is shown in Figure 1.1.[6]

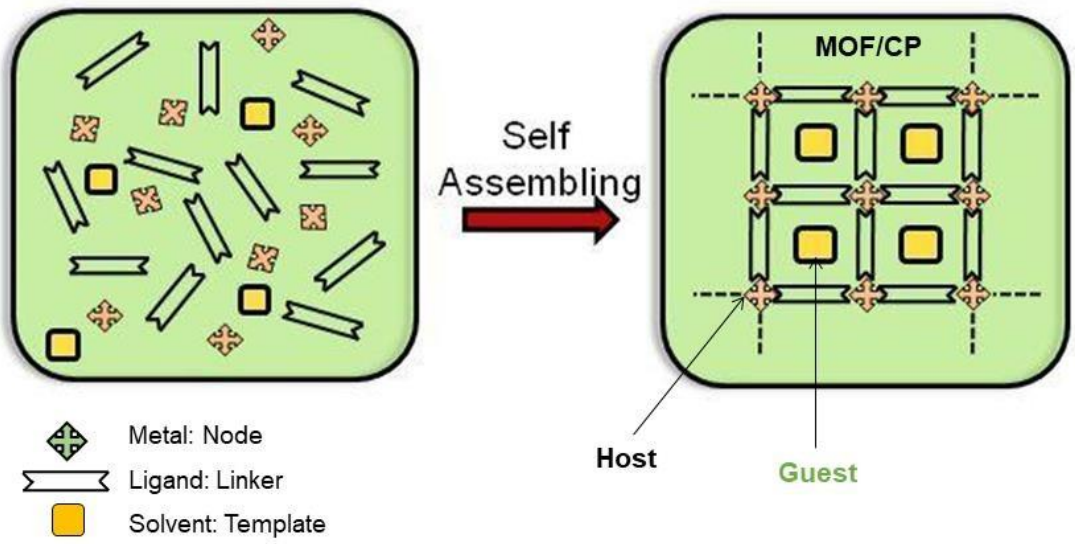

Figure 1.1. Self-assembling process of a MOF.[6]

Generally, metal ions have more than one vacant and labile site, which allows multi-conformations; thus, infinite extended polymeric 1D, 2D or 3D or discrete (0D) structures can be formed. Transition metal ions are widely used in MOFs, such as Cu^{+}, Cu^{2+}, Ag^{+}, Zn^{2+}, $Co^{2+,}$ and Ni^{2+}; they attract considerable interest due to their stability, porosity and synthetic versatility. The sketch diagram of the building blocks in a MOF's synthesis is represented in Figure 1.2.[7]

In terms of ligands, a flexible ligand can give different conformations that could lead to a difficult prediction of the framework's geometry. On the other hand, rigid ligands are suitable for achieving good topological prediction.

4-4'-bipyridine is a typical rigid bidentate ligand; though the carbon bond between two aromatic pyridine rings can rotate, the orientation of this pair of rings does not change. Following this concept, many ligands can be classified as rigid, such as 2,4,6-tris-(4-pyridyl)pyridine (TPP) and 2,4,6-tris-(4- pyridyl)benzene (TPB), both of them are tridentate no matter the rotation of C-C bond .[8]

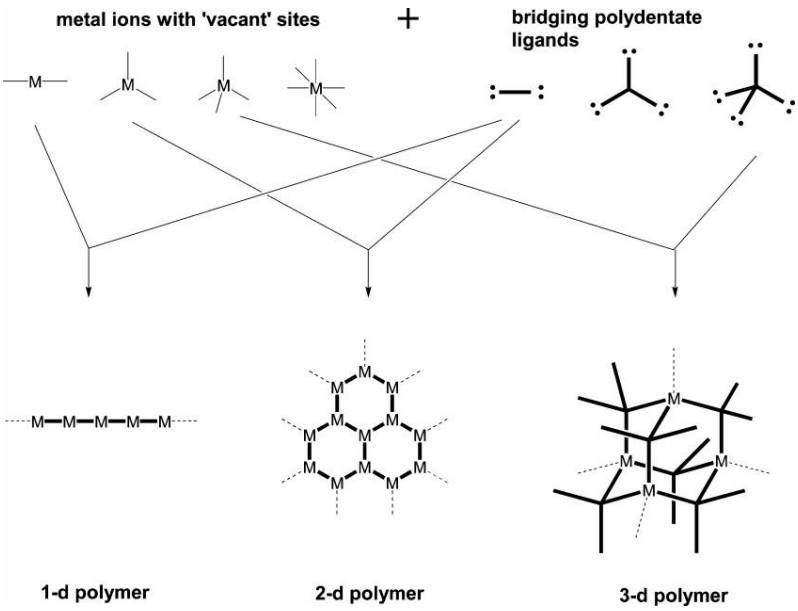

Figure 1.2. Sketch diagram of building block in the synthesis of MOFs.[7]

1.1.2 Synthesis method

The synthesis of crystalline MOFs is commonly carried out in the solution state under harsh conditions. Among the main methods, solvothermal/hydrothermal synthesis is the most common as it produces large crystals of good quality. Solvent stratification is also a good crystallization method, often giving mixtures of crystals due to the milder temperature conditions that allow the formation of kinetic and thermodynamic products.[9]

Mechanochemical synthesis is the method that is exploited for the solid-state synthesis of MOFs, which is very important to reduce the amount of toxic solvents used to dissolve the reagents for the self-assembly process. For the first time, an investigation applying mechanochemical synthesis on $M_{12}L_8$ poly-[*n*]-catenanes was carried out by Martí-Ruja's research group.[10] An amorphous phase product consisting of tridentate ligand (30mg TPB (2,4,6-tris-(4-pyridyl)benzene) as organic linker and $ZnBr_2$ (34 mg) was obtained by grinding them for 15 minutes using a mortar and a pestle. The product

is not crystalline, which means that full structure elucidation cannot be carried out using *ab initio* PXRD. Immersing and stirring for 20 h the amorphous product into 6 ml 1,2-dichlorobenzene yielded a solid powder that after filtering the suspension, shows a transformation from an amorphous phase to a crystalline as demonstrated by PXRD. Fortunately, by comparing the PXRD pattern against the product, with that of the product obtained from the instant synthesis (*i.e.*, using aromatic templating agents) shows that the catenanes were formed. TG analysis evidenced that the weight loss is 24.1% at 250°C, corresponding to the release of 1,2-dichlorobenzene, thus, strongly proving the formation of the $M_{12}L_8$ poly-[*n*]-catenanes as an amorphous phase by grinding without templating solvent.

1.2 Poly-[*n*]-catenanes

Interlocked molecules that contain one or more mechanical bonds have been identified in biomacromolecules, such as catenated circular DNA and protein chainmail. [11] Poly-[*n*]-catenanes are a class of polymer chains consisting of mechanically interlocked molecular rings without any covalent spacer. The '*n*' indicates the number of concatenated rings or cages. The topological mechanical bonds between adjacent molecular fragments that are linked together can offer a significant degree of freedom and mobility about the catenane moieties.[12,13]

1.2.1 Structure of catenanes

Poly-[*n*]-catenanes have raised much interest due to their high strength and flexibility. Several poly-[*n*]-catenane chain conformations are present compared to covalently connected molecules. The multiple conformations can provide opportunities to access polymeric materials and exhibit specific properties including dynamic aspects. Different types of poly-[*n*]-catenanes are shown in Figure 1.3.[14]

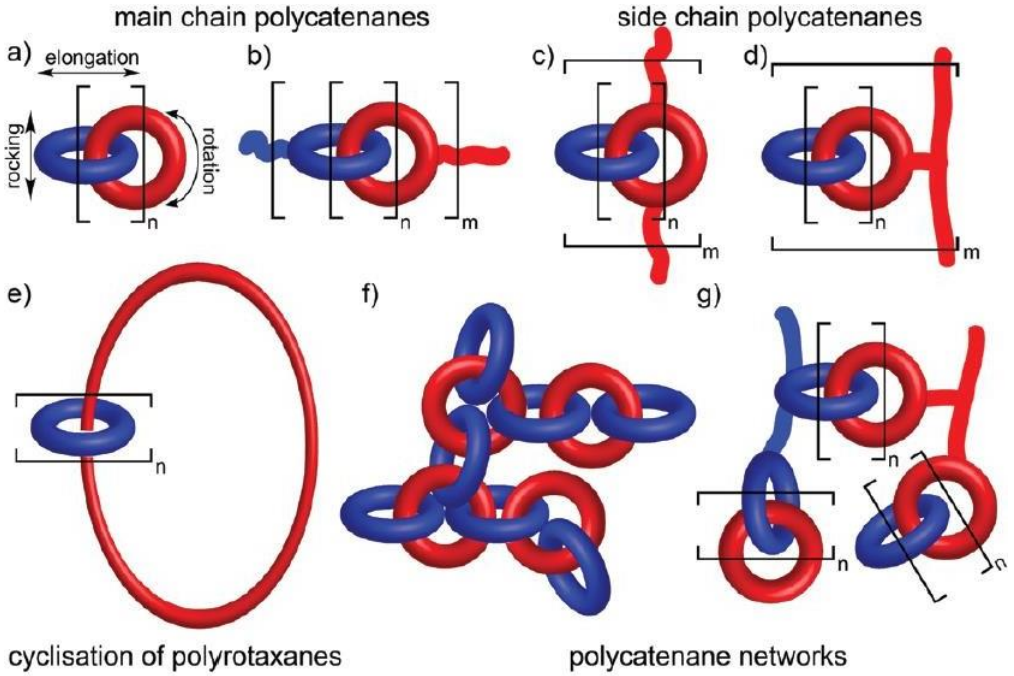

Figure 1.3. Cartoon representation of different types of poly-[*n*]-catenane.[14]

Generally, the chain conformations of poly-[*n*]-catenane are classified into four types: (*i*) main chain poly-[*n*]-catenane. (*ii*) side chain poly-[*n*]-catenane. (*iii*) cyclization of polyrotaxanes. (*iv*) poly-[*n*]-catenane networks. Figure 1.3. (a) demonstrates three unique mobilities that exist in poly-[*n*]-catenane compared to covalently connected molecules.The parallel length change between two adjacent gravity centers of rings is called elongation; when the ring rotates at its plane is called rotation; and if the ring moves perpendicular to its plane is called rocking. [15,16,]

1.2.2 Synthesis method of catenane

Currently, the most common way to synthesize catenanes is to utilize a templating method to ensure that the individual components are appropriately positioned. Such templating can be introduced by designing non-covalent interactions into the initial compounds.[17] Thus, they self-assemble specifically and facilitate the catenane formation—such non-covalent interactions, including but not limited to metal-ion interactions, hydrogen interactions, aromatic π-π interactions, and host-guest interactions.[18] The most common ways to prepare mechanically interlocked molecules are shown below:

(1) Metal-ion interactions are also called transition-metal (TM) templating. TM templating method uses the nature of the transition metal ion to coordinate with a circular ligand and a linear chain ligand which can pass through the cycle. After this coordination step, the chain ligand into a ring can be easily closed. Therefore, an interlocked macrocycle is formed (Figure 1.4).

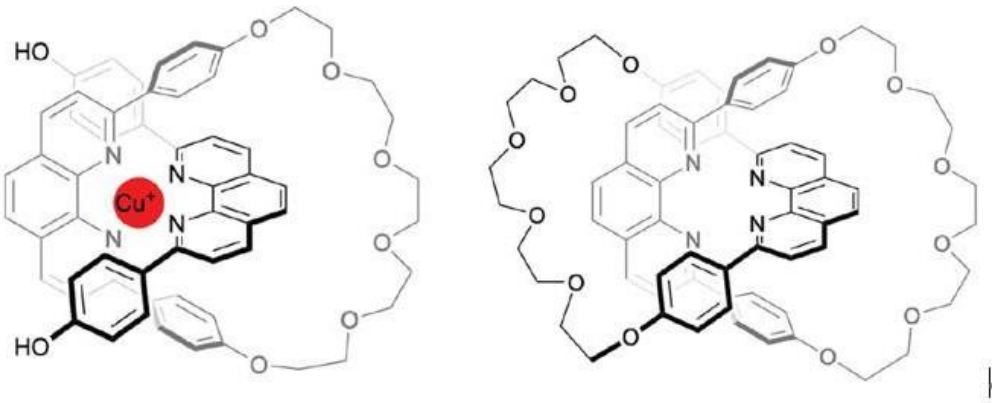

Figure 1.4. Catenane formed using the TM method.[14]

(2) Electrostatic π-π interactions are also intensively used to access interlocked catenanes. The ligand with the electron-poor aromatic component can be incorporated into another ligandwith π-electron-rich aromatic units. Stoddart and coworkers reported an example were a π- electron-accepting macrocycle cyclobis (paraquat-*p*-phenylene) (R-CBPQT^{4+}) interlock with the electron-rich ligand (DNP38C10-Five dioxynaphthalene[38]-crown-10) by π-π interactions (Figure 1.5).[14]

(3) Besides, the successful synthesis of $M_{12}L_8$ poly-[*n*]-catenanes by the group of Martí-Rujas and coworkers, also exploit the π-π interactions between adjacent $M_{12}L_8$ cages (Figure 1.6). Infinite icosahedral cages consisting of TPB ligand and $ZnCl_2$ are interlocked forming rigid linear 1D chains. The π-π interactions arising from the aromatic central part and the templating solvent molecules are crucial for the formation. Both the mobility of pyridine rings and benzene rings are examined by ^{13}C solid-state NMR.[10]

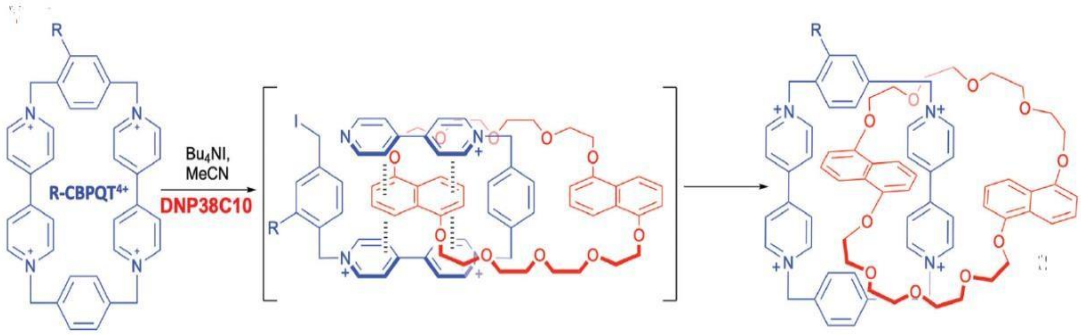

Figure 1.5. R-CBPQT^{4+} interlock with (DNP38C10).[14]

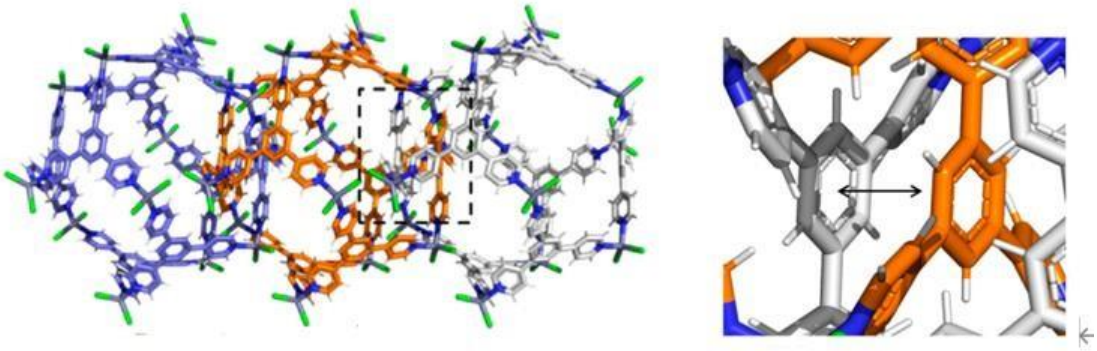

Figure 1.6. $M_{12}L_8$ poly-[*n*]-catenane, the π-π interactions between two benzene rings marked as an arrow.[20]

(4) Hydrogen interactions employed in the catenane synthesis are usually in the form of X-H…Y, where Y represents Halogen atoms. The Halogen atom forms a hydrogen bond with the hydrogen atom, which is connected with other atoms by a covalent bond. Paul D. Beer and co-workers introduced an anion-templated method to synthesize a catenane which is applied for anion recognition (Figure 1.7).[19]

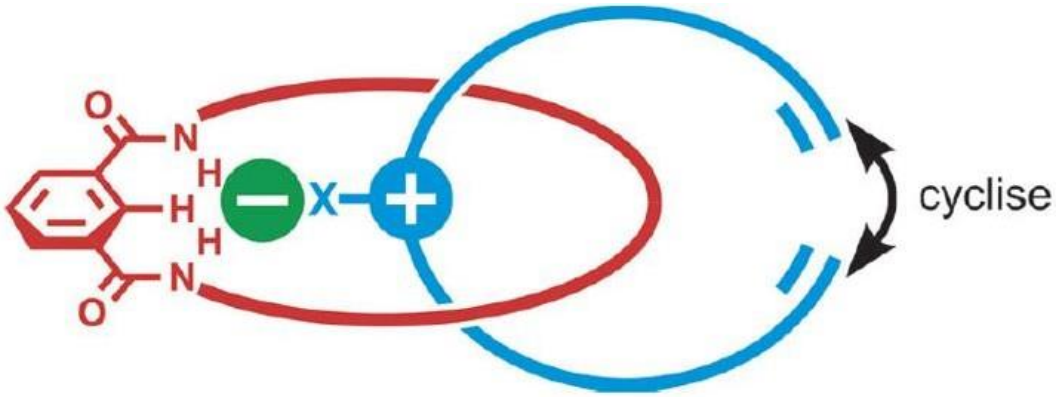

Figure 1.7. Cartoon representation of orthogonal pseudorotaxane species, inwhich X is a halogen atom.[19]

1.2.3 A case study of $M_{12}L_8$ poly-[*n*]-catenanes

In the past months, we have focused on synthesizing $M_{12}L_8$ poly-[*n*]-catenanes based on ligand TPB and Zn(II) salts, at the same time, we have exploited host-guest properties such as molecular guest inclusion and separation.[10]

$M_{12}L_8$ poly-[*n*]-catenanes have been successfully synthesized both in the crystalline and amorphous phases. Single-crystal X-ray crystallography revealed the structure of $M_{12}L_8$ poly-[*n*]-catenanes made from TPB and $ZnCl_2$ by slow crystallization method with the templating solvent nitrobenzene. [20] A discrete $M_{12}L_8$ nanocage with 8 faces occupied by ligand TPB and the remaining 12 triangular faces opened formed an icosahedron. Guest nitrobenzene is included and ordered in the host cage arranged in a hexagonal symmetry. This order is due to good electrostatic interactions between the pyridine group and the electron-rich aromatic ring in nitrobenzene molecules. Electrostatic $Zn{-}Cl\cdots H{-}C_{aromatic}$ interactions between a non-interlacing neighboring $M_{12}L_8$ nanocage and the nitrobenzene also contribute to making the guest molecules ordered. This poly-[*n*]-catenane consisting of an infinite number of $M_{12}L_8$ nanocages which are interlocked forming one-dimensional chains.

Of our interest was to investigate the effect of subtle changes in the tridentate ligand, like substituting the central aromatic ring, for instance in a fully pyridinic ligand. Although work had been done already by Dehnen and Constable,[28] the interest herein was also to study their solid-state reactivity as well as the kinetic control using fast crystallization methods.

The aromatic-aromatic interactions are crucial to the formation of crystalline poly-[*n*]-catenane. This point can be reflected by the because TPB can form a good amount of single crystals with Zinc salts by layer method (*i.e.*, slow crystallization), while TPP yields less single crystals and of lower quality.

The reaction of TPB/TPP and Zn(II) salts is a kinetically controlled reaction. Besides the slow crystallization reaction, we can obtain an amorphous product made from TPB and Zn(II) salts in a solid-state reaction within 15 minutes. From our latest results, we ground TPB and Zn(II) salts (X=Br, Cl, I) with a proper ratio in a mortar. After 15

minutes, the obtained products were measured by PXRD, and all of then showed an amorphous phase. However, after a gas-solid reaction, we can see a transformation from amorphous into crystalline by immersing the amorphous produdct into a templating solvent 1,2-dichlorobenzene (Figure 1.8). Compared the crystalline PXRD data to the simulated PXRD data from the single-crystal poly-[*n*]-catenane we mentioned above, we can find they are highly overlapping. TG analysis also proved the presence of 1,2-dichlorobenzene in the crystalline products. Thus, we realized the synthesis of poly-[*n*]-catenanes in an amorphous phase. Additionally, a transformation into a crystalline phase can be realized by the effect of templating solvent. [10]

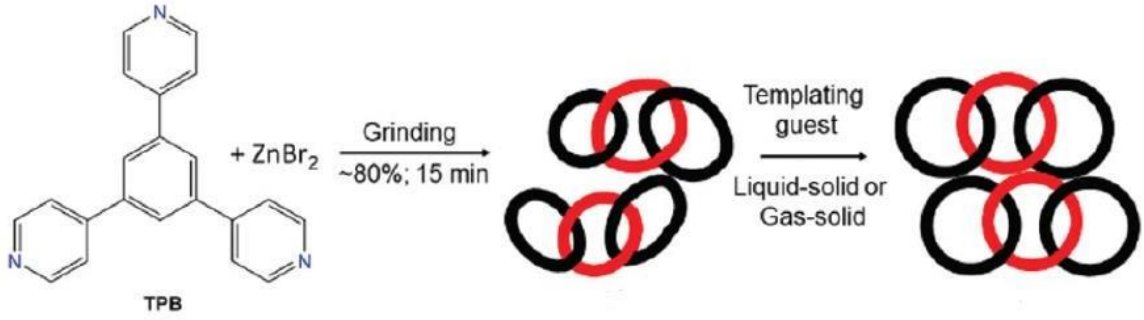

Figure 1.8. Cartoon representation of the phase transformation.[10]

1.3 0-Dimensional Metal-Organic Cages

In the past decade, many complex 3-D molecules were self-assembled by non-covalent bonds. Coordination self-assembly via *molecular paneling* is one of the strategies among all non-covalent forces to reach 3-D molecules. The final product's structure depends on the molecular panel consisting of metal ions and organic ligands.[21] Compared to metal-organic frameworks (MOFs), metal-organic cages (MOCs) equipped with larger internal voids and cavities are 0D structures that do not extend in the 3D. Importantly the ability to encapsulate guest molecules in the solution state is outstanding. However, the guest behavior of 0D in the solid state is much less studied.

1.3.1 square planar and organic ligands

As we mentioned above, the structure of the final MOCs depends on the structure of the subset of organic molecular panels. Therefore, a well-defined panel can help us deduce the structure of the target MOCs. Molecular panels consist of coordination metal ions and organic ligands; if we fix the angle of the coordination metal ions and the geometry of the organic ligand, it can show us a particular shape of the panel.[22,23]

Fujita introduced the concept of square planar by incorporating 90° coordination angles of transition metals into metal-organic complexes. [24] An ethylenediamine-protected Pd(II) complex with non-distorted 90° bond angles was prepared, and due to the cis-protection, the coordination nature of the metal ion changes from divergent to convergent. 4,4'-bipyridine is a rectangular ligand with two nitrogen atoms on both sides which can coordinate with the transition metal ion Pd. One Pd(II) complex coordinates with one 4,4'-bipyridine ligand to form a single rectangular panel. By considering the number of free coordination bonds, we can deduce a product with a square shape (Figure 1.9).[25]

Figure 1.9. Cartoon representation of Pd(II) complex and 4,4'-bipyridine. [24]

1.3.2 Structure rises from 1-D to 3-D

Based on the theory of molecular panels, the construction of MOCs is like 'building blocks.' The shape of organic ligands can be defined by their planar structure. For example, 4,4'-bipyridine is a 'rod,' a class of organic ligands with the same planar structure (1-D linear chain) but different coordination points that can also be assumed as 'rod' (Figure 1.10). 2,4,6-tris(pyridine)-benzene (TPB), 2,4,6-Tris-(4-pyridyl)-pyridine (TPP), and 2,4,6-Tris(4-pyridyl)-1,3,5-triazine(TPP) are a class of 'tridentate' ligands and can be assumed as triangle panels (Figure 1.11).

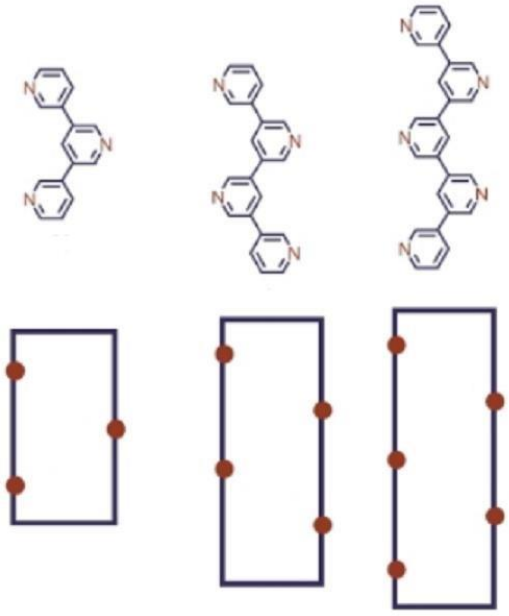

Figure 1.10. Cartoon representation of the shape of a class of 'rod' ligands.[31]

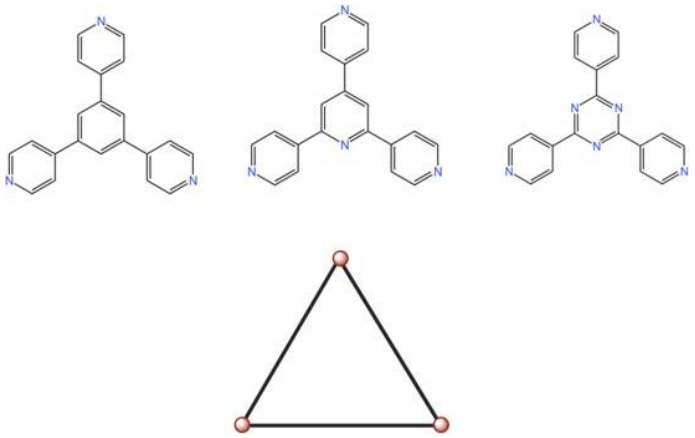

Figure 1.11. Cartoon representation of the shape of a class of triangular ligands.[24]

Once the shape of the ligands and the angle of the coordination metal ions are judiciously selected, we can deduce the structure of the final self-assembly product. The following figure 1.12 a) shows a 1-D rod to 2-D molecules and 1.12 b) shows a 2-D panel to 3-D molecules. [26]

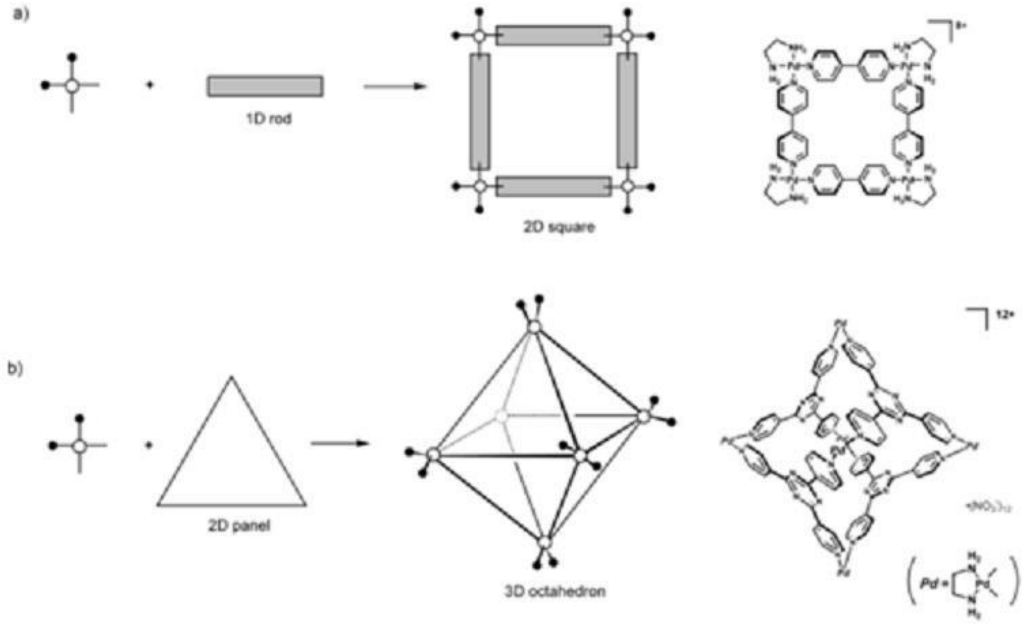

Figure 1.12. Cartoon representation of the process from 1-D to 2-D and 3-D. [24,25]

2 Results and discussion

2.1 Poly-[*n*]-catenane of $M_{12}L_8$ (TPP and Zinc halides)

Poly-[*n*]-catenanes of MOCs are a class of Mechanically Interlocked Molecules (MIMs). The structure of a poly-[*n*]-catenanes can be considered the molecular equivalent of a macroscopic chain shown in Figure 2.1. They are attracting increasing attention becausewe can combine the properties of MOCs and MOCs by preparing poly-[*n*]-catenanes of interlocked MOCs. Therefore, research in this area has been carried out by Martí-Rujas, et al. by using *exo*- tridentate ligand TPB/TPP and Zn(II) salts.

Figure 2.1. Chain of poly-[*n*]-catenanes.[32]

2.1.1 A case study of one-dimensional poly-[*n*]-catenanes (TPP and $ZnCl_2$) [27]

There are few reports of infinite mechanical interlocked coordination cages so far. One of such case reported by Dehnen group is a one-dimensional linear chain of poly-[*n*]-catenanes made from coordination cages based on the tridentate ligand 2,4,6-tris(4-pyridyl)pyridine (TPP) and $ZnCl_2$.[28] They prepared the product by layering method, 5.0 mg TPP dissolved in 10 ml chloroform as the bottom layer, a 5 ml methanolic solution with 6.6 mg $ZnCl_2$ as the top layer, and crystal collected three weeks later. The structure was determined by single crystal X-ray diffraction, which showed to be the polycatenane with molecular formula $[(ZnCl_2)_{12}(TPP)_8]_n$ $xCHCl_3$.

The $[(ZnCl_2)_{12}(TPP)_8]$ ($M_{12}L_8$) nanocage is an icosahedral structure consisting of eight trigonal plates in which $ZnCl_2$ units at each of the 12 vertexes and eight TPP ligands connect all $ZnCl_2$ units. Infinite $M_{12}L_8$ connected by mechanical bond instead of any direct bonding interaction and formed one-dimensional(1-D) interlocked poly-[*n*]-catenanes along the crystallographic *c* axis (Figure 2.2). Such mechanical bonds contributed from both core ligand interaction and host-guest interaction.

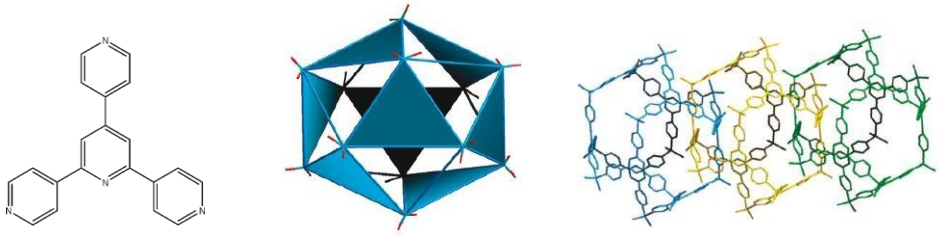

Figure 2.2. Structures of TPP; a single cage of $M_{12}L_8$; interlocking $M_{12}L_8$ cages.[28][10]

2.1.2 Instant synthesis of TPP and zinc halides

As mentioned above, the single crystal structure of the $M_{12}L_8$ poly-[*n*] -catenane using TPP was already reported, but there is not report of the synthesis under kinetic control. Instant synthesis is extremely fast crystallization method, which means the reaction take place instantaneously yielding crystalline products. 2,4,6-Tris-(4-pyridyl)pyridine (TPP) is a tridentate ligand very similar to 2,4,6-Tris-(4-pyridyl)benzene (TPB), with a nitrogen atom substituting the carbon atom in the central benzenic part decreasing the spatial distribution of electron density. Thus, even if the TPP single crystals poly-[*n*]-catenane were successfully formed with $ZnCl_2$ and ZnI_2, the feasibility of instant synthesis using $ZnBr_2$ still cannot be anticipated. Two main factors contribute to the $M_{12}L_8$ self-assembly process: the core ligand interaction and the templating guest. To provide the host-guest interaction, we selected 1,2-dichlorobenzene as a templating guest. TPP (30 mg) were mixed with 10 ml 1,2-dichlorobenzene, and an additional 4 ml methanol were added and stirred in a flask for 5 mins at room temperature until the suspension became clear. Then, a methanolic solution made from 33mg $ZnBr_2$ and 2 ml methanol was added to the flask in a second. After the addition of the metallic solution, a precipitate was formed immediately. The reaction lasted for the 30s. Then the product was collected by filtration. The white powder (2-o-DCB) was 55 mg

corresponding to a 60% yield. (Figure 2.3)

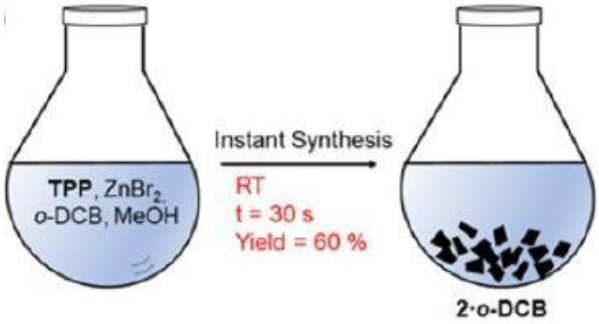

Figure 2.3. Instant synthesis of TPP and $ZnBr_2$ forming 2-o-DCB. [27]

Then, the product was left in the atmosphere for five days to make sure it was completely dry and then analyzed by powder XRD (Figure 2.4).

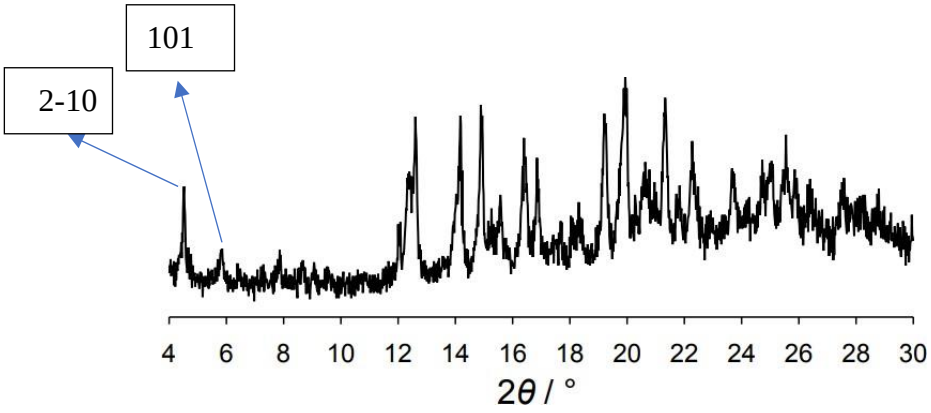

Figure 2.4. Powder XRD pattern of the sample(2-o-DCB). [27]

The 2-o-DCB diffractogram demonstrates that the sample is crystalline, especially two reflections marked as 2-10 and 101, that correspond to the reticular planes cutting the aromatic- aromatic TPP interactions in the poly-[*n*]-catenane the quadruple peaks(reflections) ranging from 18-23 2θ / ° also indicated the catenane structure, in particular, the $M_{12}L_8$ cages. Significantly, the pattern is highly overlapping with the pattern of poly-[*n*]- catenane made from TPB and $ZnBr_2$ shown in Figure 2.5. Thus, the structure of the $M_{12}L_8$ poly-[*n*]-catenane can be confirmed according to the PXRD data. Thermogravimetric (TG) analysis has shown the weight decrease to 64% at 300K, which means that there was a 36% of weight loss is due to the guest release (Figure 2.6). Besides, the solvent can still be measured included inside the cage after 5 days at room temperature due to the void of each $M_{12}L_8$ being separated. This means that there

are no continuous channels. Good thermal stability is observed, indicating that the structure remains up to 300℃.

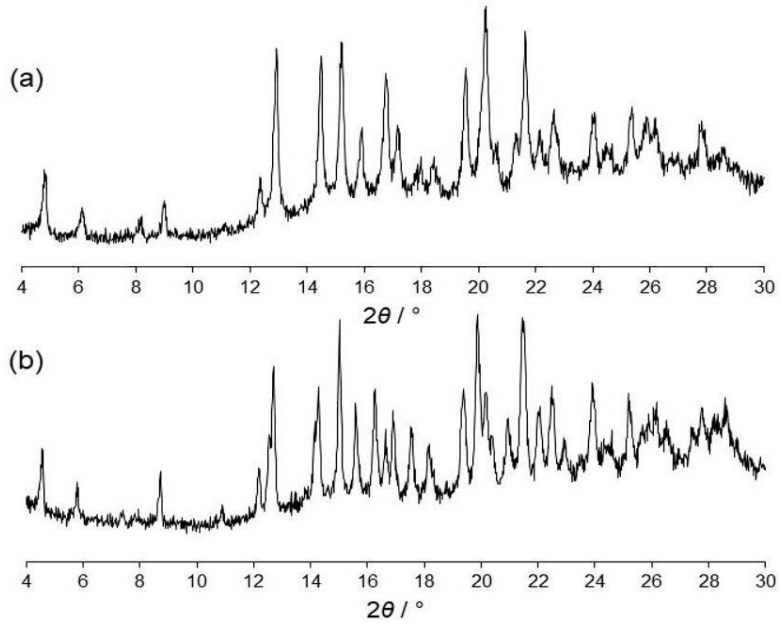

Figure 2.5. Comparison between TPB based poly-[*n*]-catenane and white powder(2-o-DCB), a is TPB based poly-[*n*]-catenane, b is white powder(2-o-DCB). [27]

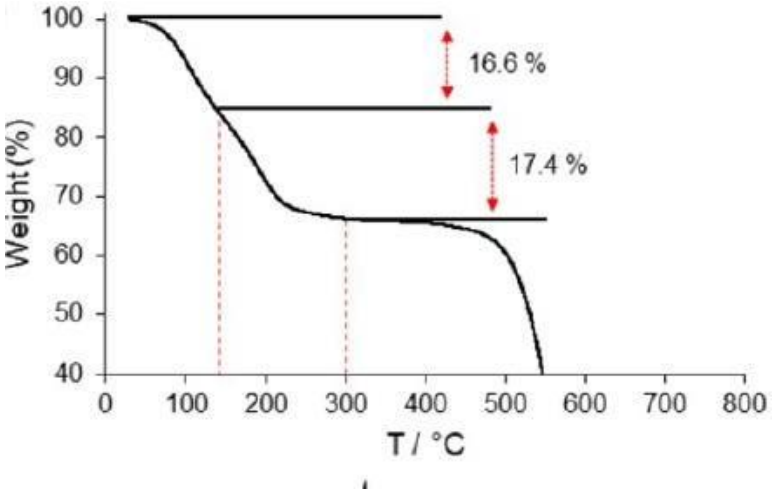

Figure 2.6. TG analysis of white powder(2-o-DCB). [27]

Since the poly-[*n*]-catenane was successfully formed by the instant synthesis of TPP and $ZnBr_2$, we wondered if such a method also works for ZnI_2 and $ZnCl_2$. Following the same process, TPP (30 mg) dissolved in 10 ml 1,2-dichlorobenzene and additional 4ml methanol and added a solution made from 47mg ZnI_2 with 2 ml methanol;

TPP (30 mg) dissolved in 10 ml 1,2-dichlorobenzene and additional 4 ml methanol and added a solution made from 20 mg $ZnCl_2$ with 2 ml methanol. After filtration, two products were obtained which amount is 68 mg and 49 mg respectively. From the pattern of PXRD, all characteristic peaks fit the structure of poly-[*n*]-catenane and overlap with the previous pattern, which confirmed a catenane structure (Figure 2.7). Importantly, the $ZnCl_2$ powder gives a material with better crystallinity, suggesting that the halide in the structure has an important role considering the intermolecular forces that contribute to the stabilization of the 1D chains of interlocked MOCs.

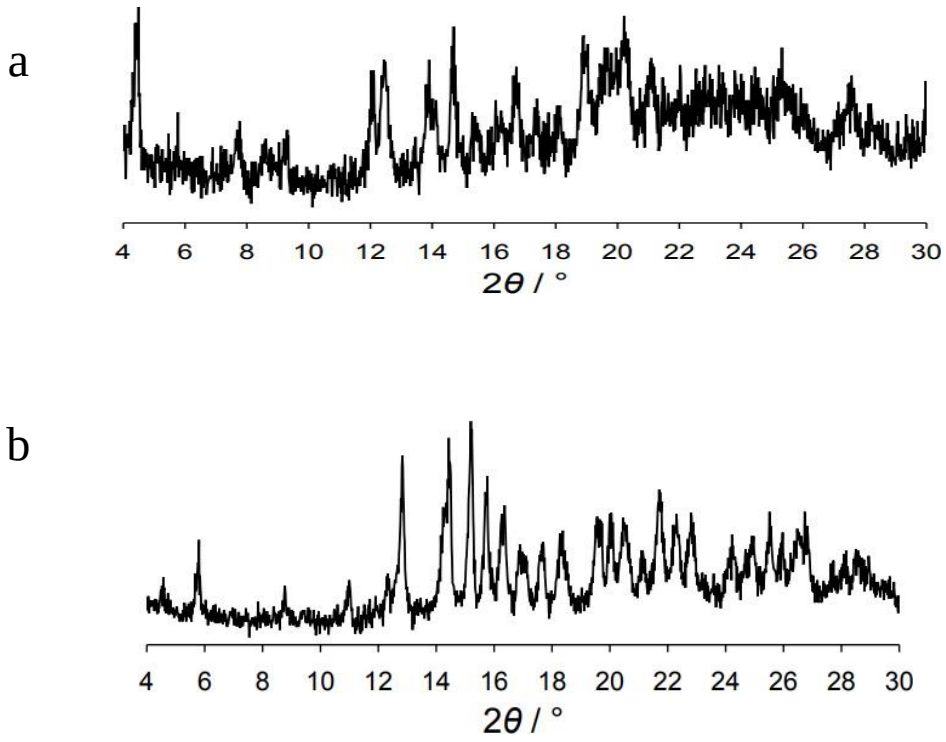

Figure 2.7. a: PXRD pattern of instant synthesis product of TPP and ZnI_2. b: PXRD pattern of instant synthesis product of TPP and $ZnCl_2$. [27]

2.1.3 Solid-state reaction and transformation from the amorphous phase to the crystalline phase

Molecular movement in the solid state was proved by Koichi Tanaka.[29] Based on the theory of mechanochemistry, a reaction without solvent benefits both the yield and the environment. Non-recyclable, toxic solvents have a negative influence on the chemical industry. Thus, we attempted to prepare poly-[*n*]-catenane of TPP and zinc salts in the solid state by grinding with a pestle and mortar.The neat grinding method aims to form a product by manual grinding with the help of a mortar and pestle or by means of mechanical milling which includes ball milling and vibratory millwithout the addition of a solvent. Using a mortar and a pestle TPP (30 mg) were ground with 47 mg ZnI_2 for 15 minutes in order to mix the reactant homogeneously by neat grinding. The final product is a light-yellowpowder, left the final product to equilibrate with the atmosphere for 1 day after being washed with MeOH (4 ml) and chloroform (4 ml) to eliminate any unreacted species or by-product. The final amount obtained is 54 mg(70% yield).

Then, to monitor if the solid-state reactivity yields the same kind of product, neat grinding was applied using $ZnBr_2$ and $ZnCl_2$ and monitored by powder XRD.

Neat grinding of TPP and $ZnBr_2$: 30 mg TPP was ground with 32.7 mg $ZnBr_2$ for 15 minutes in order to mix the reactant homogeneously. The final product is a white powder, leaving it to equilibrate with the atmosphere for 1 day after washing with MeOH (4 ml) and chloroform (4 ml). The final amount obtained is 46 mg (73% yield).
Neat grinding of TPP and $ZnCl_2$: 30 mg TPP was ground with 20 mg $ZnCI_2$ for 15 minutes in order to mix the reactant homogeneously. The final product is a white powder, leaving it to equilibrate with the atmosphere for 1 day after washing with MeOH (4 ml) and chloroform (4 ml). The final amount obtained is 35 mg (72.1% yield).

As demonstrated by PXRD, all these three patterns are an amorphous phase that lacks crystallinity and shows broad bumps, which indicates no long-range order (Figure 2.8). Also, the absence of the starting TPP ligand indicates that the reaction took place. However, the amorphous phase is hard to be characterized due to the disordered structure (*i.e.*, absence of Bragg diffraction). To know if such an amorphous phase product contains mechanically interlocked $M_{12}L_8$, our strategy is to introduce an aromatic templating solvent, and thanks to the host-guest interaction and aromatic stacking, it will be possible to reconstruct the amorphous product into a new phase

product arranged orderly in the 3-D array as a crystalline material. Then collected them by filtration and left to equilibrate with the atmosphere and measured by PXRD. The PXRD patterns clearly show the phase transformation from amorphous into crystalline (Figure 2.8) The pattern of the crystalline phase is like previous patterns from the products obtained by instant synthesis, which were proved to be poly-[*n*]-catenanes. The poly-[*n*]-catenanes characteristic peaks are the 2-10 and 101. The result indicates that the mechanical bond is also formed in the amorphous product by neat grinding. The isostructural $M_{12}L_8$ poly-[*n*]-catenanes can be reconstructed by trapping aromatic solvent showing a crucial dynamic behavior via an amorphous-to-crystalline transformation.

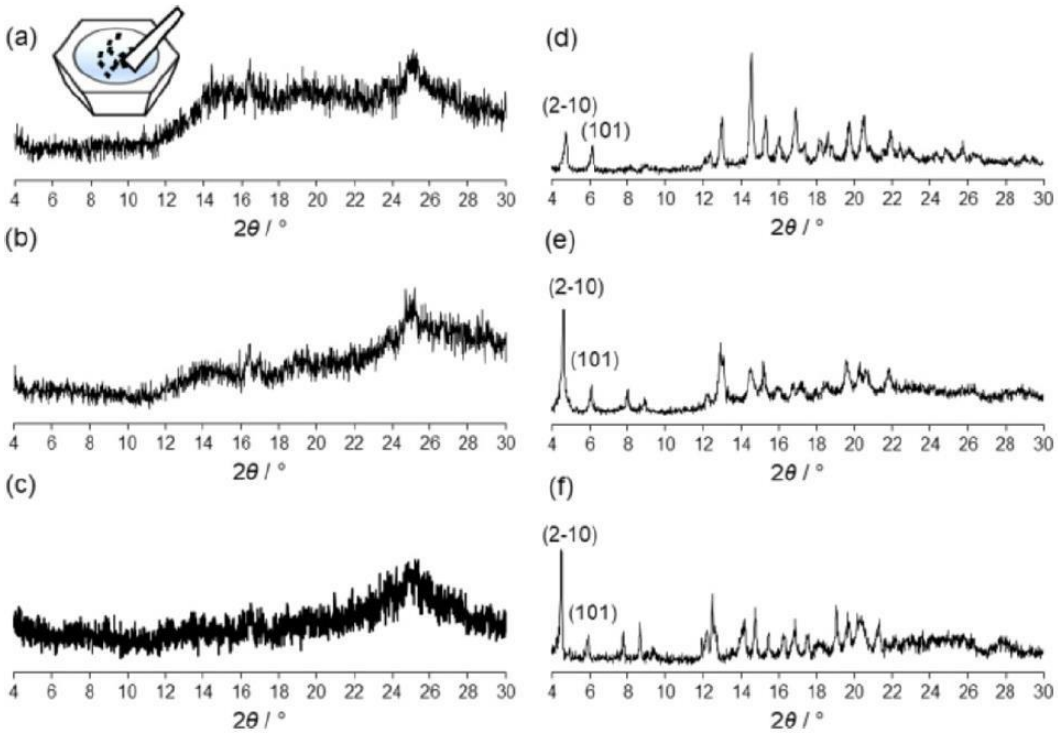

Figure 2.8. PXRD pattern of neat grinding products of TPP and ZnI_2 (a), $ZnBr_2$ (b),$ZnCI_2$ (c) PXRD pattern after immersed amorphous product of TPP and ZnI_2 (d),$ZnBr_2$ (e), $ZnCI_2$ (f) into the aromatic templating solvent.[27]

2.2 Zero-dimensional (0D) metal-organic cages(MOC)

A discrete MOC can be classified as a zero-dimensional (0D) structure which means that no extended structures are formed. There are many strategies for building discrete MOCs. The method we applied is molecular paneling via coordination. Any organic ligands with binding sites in specific geometry can be considered molecular panels; these panels can be connected by square planar which a central atom is surrounded by constituent atoms and form the corners of the square on the same plane. The open metal sites on the square planar building block coordinate with binding sites on the molecular panels and construct a well-defined structure.

2.2.1 Synthesis of square planar complex

The idea of incorporating a 90° coordination angle of transition metal into metal-organic frameworks was given by M. Fujita more than a decade ago. Non-distorted 90° angle is stable and cannot be hybridized by other organic elements. On the view of the structure, the fixed angle can help us deduce the product's geometry. Dinitrato ethylenediamine palladium(II) ($enPd(NO_3)_2$), is widely used as a square planar to coordinate with organic ligands of several geometries.[30] Since the cis-protection, the coordination nature of the metal changes from divergent to convergent. Thus, discrete $enPd(NO_3)_2$ can efficiently generate 0D structures acting as end-capping group. When $enPd(NO_3)_2$ is brought into the water, the nitrates will be replaced by the water ligand and generate active species $enPd[(H_2O)_2]^{2+}$. The synthesis of $enPd(NO_3)_2$ is carried out in an aqueous solution with $enPdCl_2$(0.42mmol) and $AgNO_3$(0.84mmol) For the synthesis of $enPd(NO_3)_2$ 100 mg of $enPdCl_2$ were dissolved in 15 ml water, put 142 mg $AgNO_3$ into solution, and let it stir in the dark at room temperature for threedays. After three days,

the solid $AgCl_2$ was filtered out, and the residue solution was treated with a rotatory evaporator at 35 °C, leading it to concentrate to dryness. Then the resulting precipitate was recrystallized with a drop of distillation water. After six days, we obtained the final product: an orange powder.[29] The orange sample was measured by PXRD and compared with the already published structure from SCXRD. The good match of the PXRD data confirms that the $enPd(NO_2)_3$ complex was synthesized (Figure 2.9).

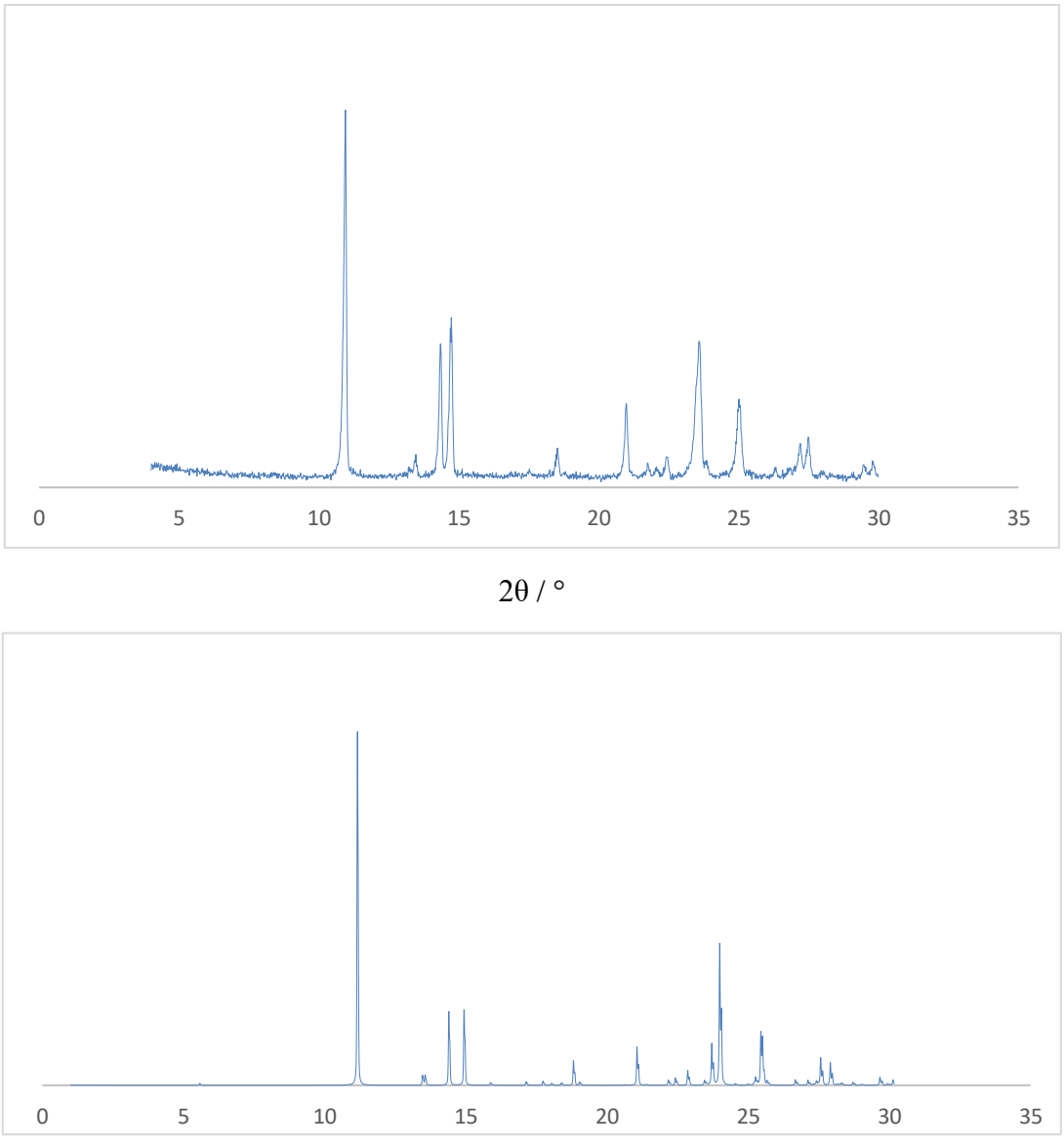

Figure 2.9. PXRD of orange powder (top) compared to simulated PXRD from CCDC (bottom).

2.2.2 A coordination square self-assembled from 4,4'-bipyridine and $enPd(NO_3)_2$

As mentioned before, a rigid organic ligand equipped with binding sites in a specific shape can be assumed as a molecular panel. 4,4'-bipyridine is a typical rectangle shape ligand with two nitrogen atoms that can coordinate with open metal sites such as the ones in the $enPd(NO_3)_2$ complex. Based on the geometry of a rectangle organic ligand (Figure 2.10) and a square planar with a 90° coordination angle, we can somehow predict that a product will form in a square shape (Figure 2.11).

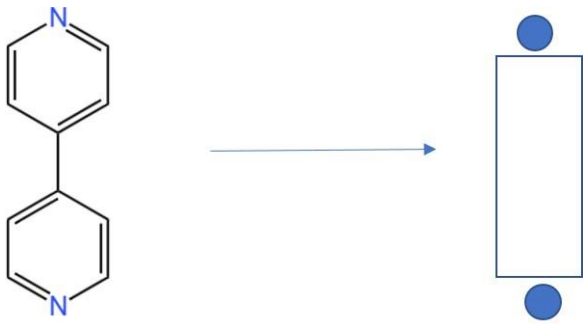

Figure 2.10. Cartoon representation of molecular panel of 4,4'-bipyridine ligand.

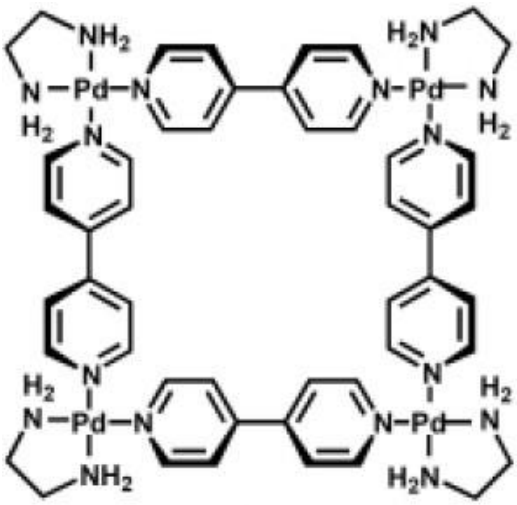

Figure 2.11. Structure prediction of 4,4'-bipyridine and $enPd(NO_3)_2$ as reported by Fujita. [25]

To determine the structure intuitively, we prepared a single crystal by layering crystallization method. 4,4'-bipyridine was dissolved in $CHCl_3$ and filled in the bottom of a crystallization tube. Then, $enPd(NO_3)_2$ dissolved in water was added dropwise as a top layer. Methanol is an intermediate layer to separate them. Especially, the ratio between 4,4'-bipyridine and $enPd(NO_3)_2$ is 1:1. After one week, large crystals suitable for single-crystal X-ray diffraction were formed after one week. The structure determined by SCXRD and is shownin the figure below. The solvent molecules were not determined due to severe disorder. Due to the 90° coordination angle of the $enPd(NO_3)_2$, each palladium atom of a square planar can link two 'rod-like' molecular panels TPB and form a forming a right angle. Utimately, a discrete square structure formed (Figure 2.12).

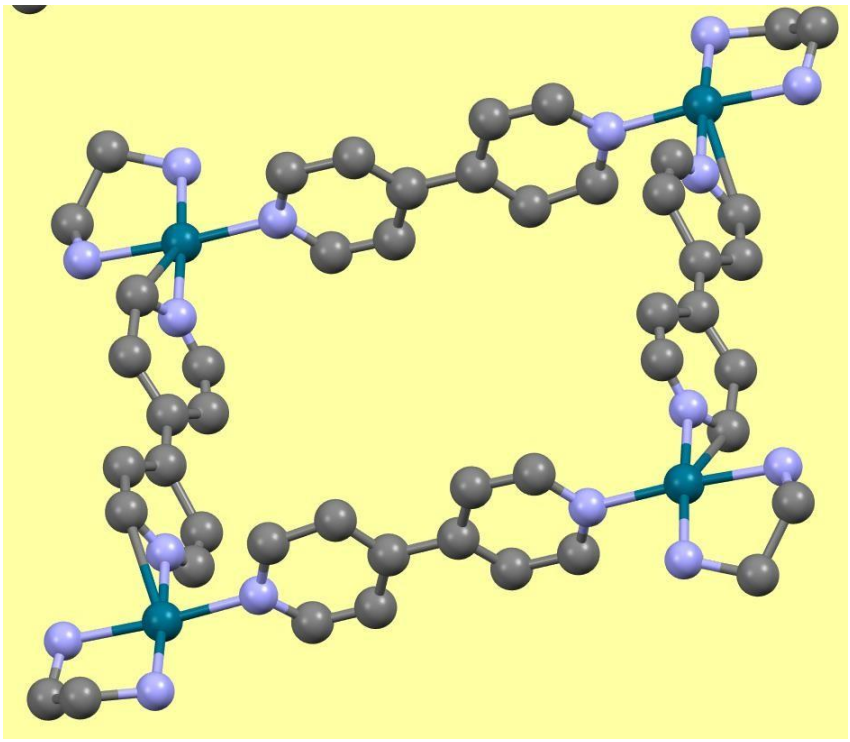

Figure 2.12. Structure of the square complex self-assembled using 4,4'-bipyridine and $enPd(NO_3)$

2.2.3 Solid state synthesis of TPB and enPd(NO_3)$_2$

Based on molecular panels, rigid TPB (2,4,6-tris(pyridine)benzene) ligand can be considered a triangular panel. Another triangle shape organic ligand that was proved successfully built an octahedral cage (M_6L_4) with enPd(NO_3)$_2$ is TPT (2,4,6-Tris(4-pyridyl)-1,3,5-triazine) (Figure 2.13). Since the TPB ligand has a benzene ring in the center, which compares to the TPT ligand, a better aromatic-aromatic interaction will be endowed. Thus, we also try synthesizing poly-[*n*]-catenane with TPB.

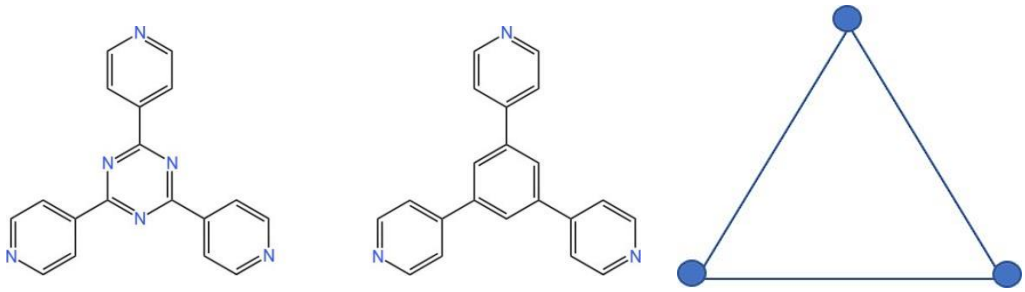

Figure 2.13. Molecular panel of TPT and TPB.

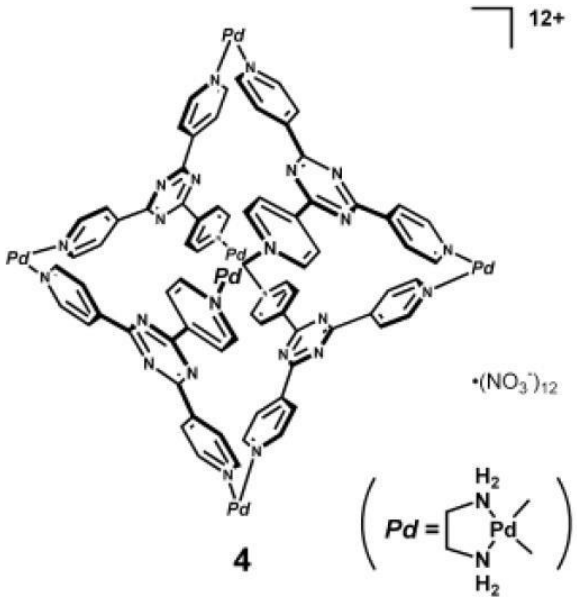

Figure 2.14. The M_6L_4 cage formed by TPT and enPd(NO_3)$_2$.[24]

To determine a structure, preparing a single crystal is always the best way, but after

several times failures, we changed our strategy from preparing the single crystal to a solid-state reaction measured by ^{1}H NMR spectra. If the TPB M_6L_4 cage forms, the structure will be similar to the octahedron cage based on TPT. (Figure 2.14) Such an octahedron cageis highly symmetry with four TPB ligands in the same environment. Thus, the NMR spectra of this M_6L_4 cage should be the same as pure TPB ligands in the aromatic range.In pure TPB ligands, there are three kinds of H protons with a 2:2:1 ratio. To carry outthis solid-state reaction, we put the reactant TPB and enPd$(NO_3)_2$ with a molar ratio of2:3 into the mortar and ground with a pestle with different reaction times. The reaction mixture were partially taken at different reaction times (*i.e.*, 5mins,15mins, 25mins, 40mins, 50mins) and measured by ^{1}H NMR (Figure2.15). Firstly, two 'TPB like' patterns with different intensities can be observed in the NMR spectra of the sample obtained from a short reaction time (less than 50 mins). At such reaction time, TPB ligands and enPd$(NO_3)_2$ are physically mixed, and the powder shows a heterogeneous phase instead of a homogeneous one. The different observed intensities can be explained by the fact that there is still a small amount of TPB ligands unreacted. Nevertheless, most TPB ligands already formed a MOC with enPd$(NO_3)_2$. The 'TPB like' pattern in weak intensity keeps decreasing as reaction time increases. When the reaction time lasts for 50 mins, only one pure TPB pattern can be observed, which fits our hypothesis of a highly symmetric octahedron M_6L_4 cage.

The aromatic part ^{1}H NMR spectra of the sample ground for 50 mins is shown below (Figure 2.16). As we can see, only one TPB pattern can be observed, and the ratio among the three peaks is 1.96:2.01:1.00, which is very close to 2:2:1, the theoretical ratio of ^{1}H spectra in pure TPB.

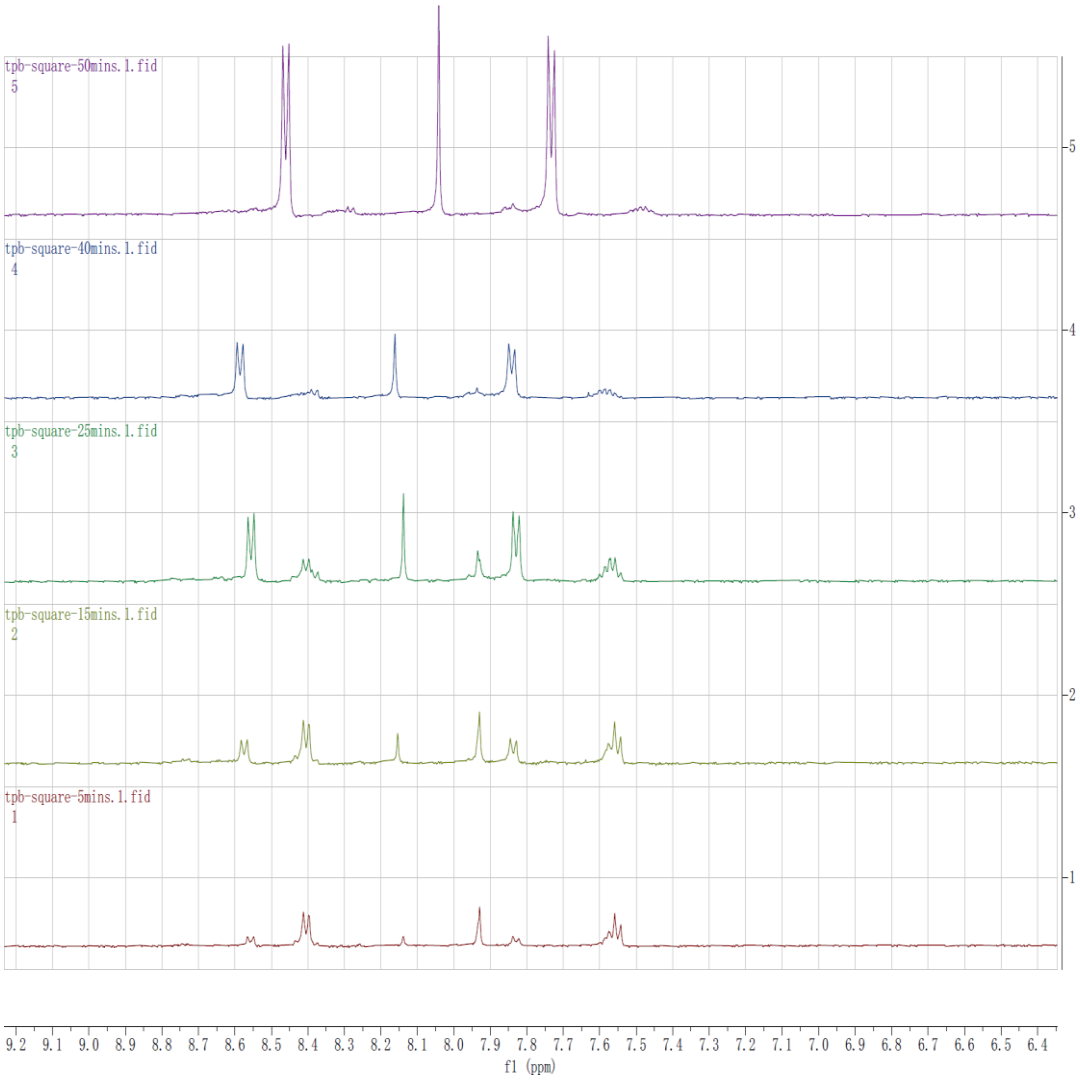

Figure 2.15. Aromatic range ^{1}H NMR spectra of samples taken at different reaction time (5mins, 15mins, 25mins, 40mins, 50mins).

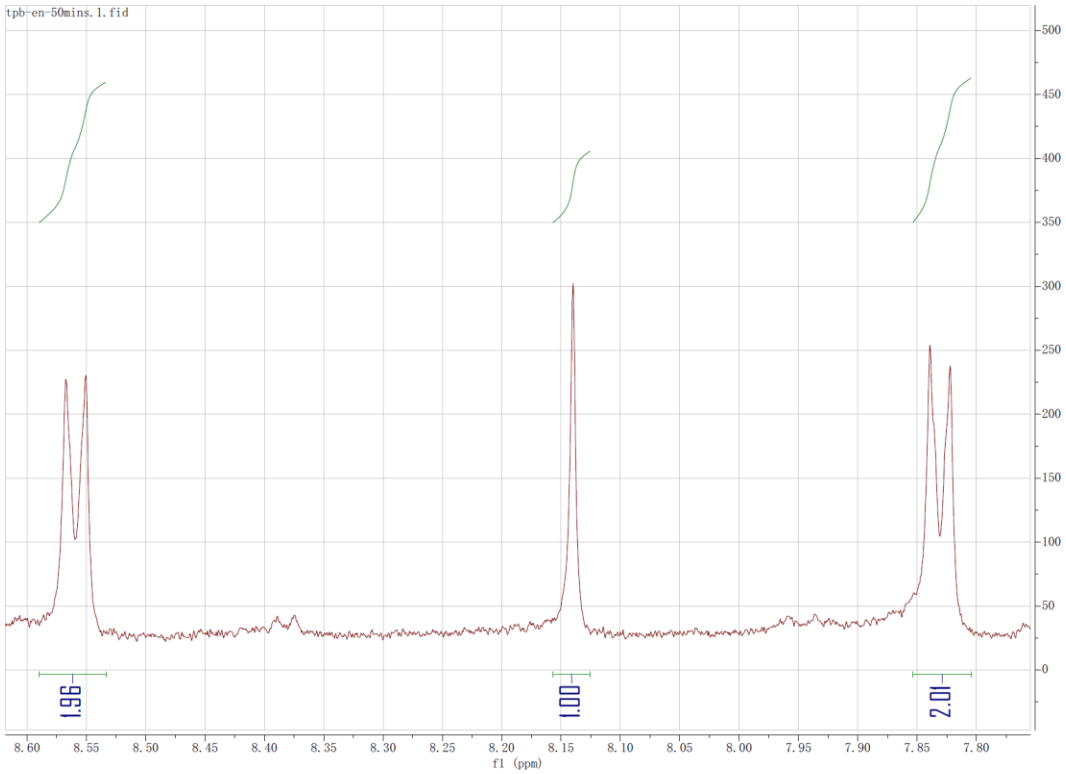

Figure 2.16. Aromatic range ^{1}H NMR spectra zoom in of samples taken at reaction time 50 mins.

The ^{1}H NMR spectra of $enPd(NO_3)_2$ are shown below (Figure 2.17), which also support the hypothesis of the formation of an octahedron MOC.

Firstly, for the non-aromatic part, we can only observe the H proton of $-CH_2-CH_2-$ belonging to the square planar. Furthermore, four H protons of $-CH_2-CH_2-$ will exist in the same environment only if the square planar link with a highly symmetric structure. And such a highly symmetric structure can be assumed as a plane and 'cut' the $-CH_2-CH_2-$ in the middle. If so, four H protons will show the same intensity under the ^{1}H NMR spectra. Corresponding to this theory, the ^{1}H NMR spectra gave us well-fit feedback. There is more than one kind of H proton that can be observed with a short reaction time (less than 50 minutes) in the range of 2.3-3 ppm. However, the sample after 50 minutes of reaction shows only one peak at 2.8 ppm, which means four H protons stay in the same chemical environment in this case.

Besides, a single peak at 2.2 ppm indicates the unreacted $-CH_2-CH_2-$. This peak can be observed among all the samples with short reaction time and finally cannot be observed when the reaction was for 50 minutes. Significantly, the disappearance of the unreacted

-CH_2-CH_2- peak is accompanied by observing a pure TPB pattern appearing in the aromatic part.

All information provided by ^{1}H NMR strongly proving the formation of an octahedron M_6L_4 MOC.

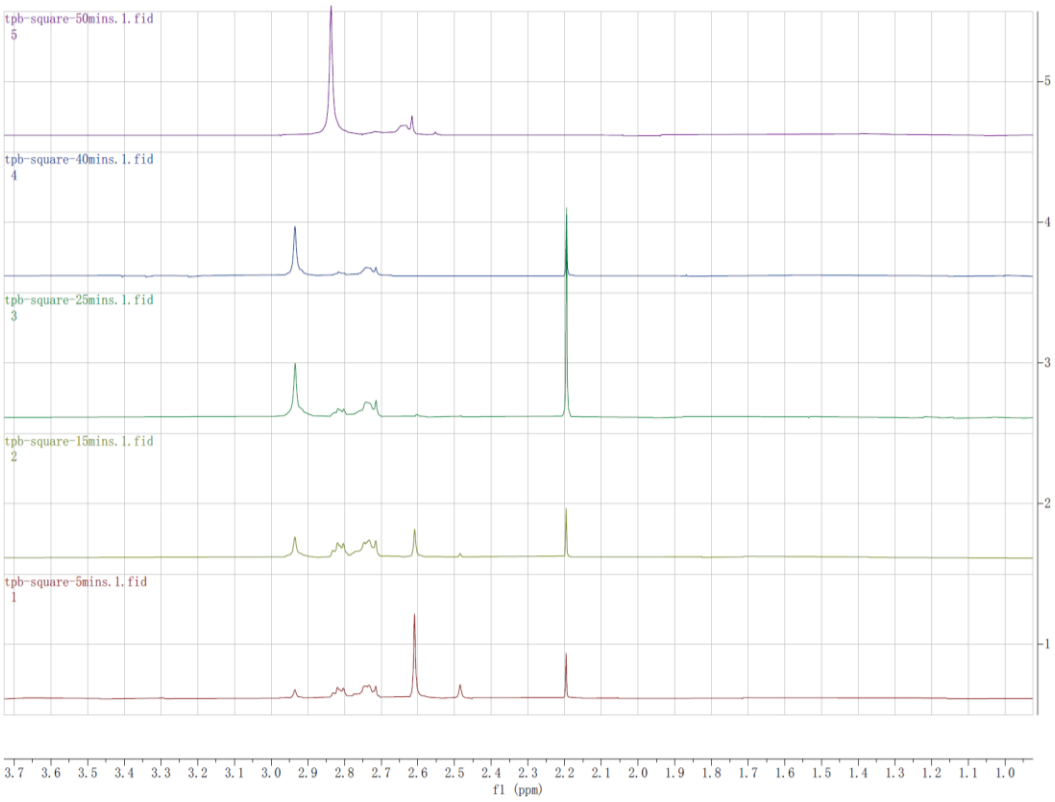

Figure 2.17. Non-aromatic range ^{1}H NMR spectra of samples taken at differentreaction times (5mins, 15mins, 25mins, 40mins, 50mins).

3 Materials and research methods

All starting reagents involved in the experiments were procured from commercial suppliers (Alfa Aesar, Apollo Scientific, Fluka, FluoroChem, Honeywell, Sigma Aldrich, TCI, iChemicals).

3.1 Analytical instruments

The following part will introduce the instruments applied in the experiments described in this thesis.

Powder X-Ray Diffraction

All the powder X-ray diffraction experiments were carried out using a Bruker D2-Phaser diffractometer equipped with Cu radiation (λ = 1.54184 Å) using Bragg-Brentano geometry. The experiments were performed at room temperature covering the $4.0° < 2\theta < 30°$ range. The sample exposure time was 2 seconds. The samples were placed on Al holders.

NMR

Bruker ARS (400 MHz) applies to all non-magnetic and non-conductive samples. Generally, the amount of sample we measured ranges from 2-3 mg. Dissolving the sample with deuterium solvents and set proper number of scans.

TGA

Thermo-Gravimetrical analyses shows the weight of a material as a function of temperature or time. The sample is heated by a controlled environment (nitrogen in our

case). The TG analyses involved in our experiments were carried out by using a Perkin Elmer Thermal Analysis instrument in the Laboratorio Analisi Chimiche at the Department of Chemistry, Materials and Chemical Engineering (Politecnico di Milano).

High-Resolution Solid-State NMR

The solid-state MAS NMR experiments were carried out on a BRUKER NEO spectrometer equipped with a commercial 4 mm MAS iProbe. The magnetic field strength was 11.74 T corresponding to a ^{13}C NMR resonance frequency of 125.75 MHz. The solid sample was packed into 4 mm ZrO_2 rotor and spun at the magic angle with a spinning speed of 12 kHz at room temperature. High-power proton decoupling (HPDEC) MAS NMR spectra were recorded after an excitation with a $\pi/2$ pulse of 3.8 μs, with a repetition time of 10 s and 1600 scans.

3.2 General procedures

3.2.1 Slow crystallization: three layers synthesis of TPB and zinc salts

Firstly, TPB (30 mg) were suspended in 8ml nitrobenzene and formed a heterogeneous suspension. Then, we added 2 ml MeOH into the suspension and keep stirring at ambient temperature until the suspension became a clear homogeneous solution. On the other hand, we prepared another solution in a vial consists of zinc salts ($ZnBr_2$ = 32.76 mg, $ZnCl_2$ = 19.83 mg, ZnI_2 = 46.43 mg) and 1ml MeOH. When these two types of solution well prepared, we set a test tube and transferred the TPB solution into it. Later, 3ml MeOH were added along with the tube wall in order to separate the TPB solution and zinc salts solution to create a biphasic. Finally, zinc salts solution was added

dropwise along with the tube wall and formed a top layer. The test tube was sealed with parafilm, and yellowish transparent single crystal formed in about 1 week.

3.2.2 Slow crystallization: three layers synthesis of 4,4'-bipyridine and $enPd(NO_3)_2$

Based on the theory of molecule paneling, the ratio between 4,4'-bipyridine and $enPd(NO_3)_2$ should be 1:1 in order to build a square complex. Thus, we add the solution of 4,4'-bipyridine (2.1 mg) dissolved in 4 ml $CHCl_3$ into the test tube as bottom layer. Corresponding, 3.85 mg of $enPd(NO_3)_2$ dissolved in distilled water (10 ml) as top layer. Additionally, 6 ml MeOH filled in the middle as a separation layer. The whole tube sealed with parafilm and stayed for about 2 weeks, transparent and colorless crystal formed in large quantity at the middle.

3.2.3 Fast crystallization of TPP and ZnX_2 (X=I, Br, Cl)

For the instant synthesis procedure, TPP (30 mg) were dissolved in the mixture of 10 ml 1,2- dichlorobenzene and 4 ml methanol, stirred at room temperature for 5 minutes until the suspension became a clear homogeneous solution. On the other hand, we prepared a 2 ml methanolic solution of zinc salts ($ZnBr_2$ = 33 mg, ZnI_2=47 mg, $ZnCl_2$ = 20 mg). The methanolic solution was added instantaneously all at once, and a precipitate was formed immediately. After filtration, we obtained the dry powder.

3.2.4 Neat grinding of TPP and ZnX_2 (X=I, Br, Cl)

Mortar and pestle were used during the neat grinding synthesis. TPP (30 mg) were ground with ZnX_2 (ZnI_2 = 47 mg, $ZnBr_2$ = 32.7 mg, $ZnCl_2$ = 20 mg) for 15 minutes. Spatulawas used to separate the solid that remained attached to the pestle and mortar to achieve

the best reactivity among reactants. The final products obtained are yellow, white and white respectively. Besides, due to the lack of solvent, all of them have an excellent yield (99%, 92.25% and 98.14% respectively).

3.2.5 Synthesis of $enPd(NO_3)_2$

The compound $enPd(NO_3)_2$ has been prepared from $enPdCl_2$ upon treatment with $AgNO_3$ in aqueous solution. Specially, in our case, $enPdCl_2$ (100 mg, 0.42 mmol) and $AgNO_3$ (143 mg, 0.84 mmol) were stirred in water (25 ml) in dark. After 3 days, AgCl white powder was filtered off, and the solution was then concentrated (rotary evaporator, 35 °C water bath) to dryness. The resulting precipitate was recrystallized from 4 ml of water and allowed to evaporate slowly at room temperature (6 days). The sample was analyzed by powder XRD and solution NMR.

3.2.6 Neat grinding of $enPd(NO_3)_2$ and TPB at different time gradient

Powder TPB and $enPd(NO_3)_2$ were placed into the mortar and ground with pestle with a molar ratio 2:3. In our case, TPB (10 mg) were ground with 9.2 mg $enPd(NO_3)_2$, followed the general procedure of neat grinding mentioned above. During the grinding, we took the sample (3 mg) away from the mortar at after 5 mins, 15 mins, 25 mins, 40 mins and 50 mins. Then, distributed these samples into five NMR tubes and dissolved in D_2O and measured by ^1H NMR.

4 Conclusions and further studies

This thesis covers two major parts I did in the past year.

The first part is the study of $M_{12}L_8$ poly-[*n*]-catenanes consisting of TPP and zinc salts. Based on the previous successful work about the synthesis of $M_{12}L_8$ poly-[*n*]-catenanes consisting of TPB and zinc salts, I started my work from neat grinding of the TPB derivative TPP and zinc salts. Amorphous products obtained from neat grinding were proved to be poly-[*n*]-catenanes by the fact that immersing these amorphous products into an aromatic solvent, the corresponding PXRD patterns changed from an amorphous to crystalline, which was overlapping well with the $M_{12}L_8$ poly-[*n*]-catenanes consisting of TPB and zinc salts. Thus, it has been confirmed that the inclusion of that aromatic solvent could work as a templating solvent contributing to the transformation from an amorphous phase to a crystalline phase via an amorphous-to-crystalline transformation.The instant synthesis method was also successfully applied to the synthesis of TPP andzinc salts, all of them are kinetically controlled, $M_{12}L_8$ poly-[*n*]-catenanes can generateefficiently in a short period.

The second part of the work has been focused on building 0-D discrete cages and squares via molecular paneling following Fujita's approach. By incorporating a 90° coordination angle of transition metal Pd into organic linkers, we can obtain a certain shape of panel, furthermore, the structure of the cage/square/cycle consisting of these panels can be deduced. 4,4'-bipyridine and enPd$(NO_3)_2$ built a square complex in single crystal by three layers method with a molar ratio 1:1. While, we observed the formation of M_6L_4 cage formed by TPB and enPd$(NO_3)_2$ as powders via mechanochemistry in the solid-state. By observing the peak shift in the ^{1}H NMR spectra of the solid product formed by grinding at different time points, it was possible to follow the evolution of the M_6L_4 formation. The ^{1}H NMR spectra provided the formation of the M_6L_4 cage, especially, the final product which was ground for 50 minutes shows a pure TPB pattern

in ^{1}H NMR.

Further work following the presented work is being focused on the crystallization of M_6L_4 to solve the X-ray structure and their potential application in molecular separation. Some functionalities of this kind of materials have been already explored. Due to the large void and highly symmetry structure, it could create a bulk condition, probably it will help us in the field of heterogeneous catalysis, molecule recognition and molecule storage, etc. Besides, we will try other types of molecular panels to build different discrete complex.

$M_{12}L_8$ poly-[*n*]-catenanes, TPB derivatives with various functional groups are being investigated by colleagues to understand how small change in self-assembling building blocks can give rise to completely diverse structures.

Bibliography

[1]R. Millini and G. Bellussi, "Properties and Applications," ed. J. Čejka, R. E. Morris, and P. Nachtigall, The Royal Society of Chemistry, ch. 1, pp. 1-36. 2017.

[2]Baumann, A.E., Burns, D.A., Liu, B. et al. "Metal-organic framework functionalization and design strategies for advanced electrochemical energy storage devices." Commun Chem 2, 86 2019.

[3]Schoedel, A., Rajeh. S, "Why Design Matters: From Decorated Metal Oxide Clusters to Functional Metal–Organic Frameworks." Top Curr Chem (Z) 378, 19 2020.

[4]O. M. Yaghi, G. Li, H. Li, "Selective Binding and Removal of Guests in a Microporous Metal-Organic Framework Nature," 378, 703-706.1995.

[5]Soumya Mukherjee, Debobroto Sensharma, Kai-Jie Chen and Michael J. Zaworotko, "Crystal engineering of porous coordination networks to enable separation of C2 hydrocarbons," Chem. Commun., 56, 10419-10441, 2020.

[6]Javier Martí-Rujas, "Thermal Reactivity in Metal Organic Materials (MOMs): From Single-Crystal-to-Single-Crystal Reaction and Beyond," Materials., 12(24), 4088, 2019.

[7]Stuart L. James, "Metal-organic frameworks," Chem. Soc. Rev. 32, 276-288, 2003.

[8]K. Umemoto, K. Yamaguchi, and M. Fujita, "Molecular Paneling via Coordination: Guest-Controlled Assembly of Open Cone and Tetrahedron Structure from Eight Metals and Four Ligands," J. Am. Chem. Soc. 122, 7150-7151, 2000.

[9]Nadeem Baig, Irshad Kammakakam, Wail Sulaiman Falath, "Nanomaterials: a review of synthesis methods, properties, recent progress, and challenges," Mater. Adv.,2, 1821-1871, 2012.

[10]Javier Martí-Rujas, Stefano Elli, Alessandro Sacchetti, Franca Castiglione, "Mechanochemical synthesis of mechanical bonds in $M_{12}L_8$ poly-[n]-catenanes," Dalton Trans., 51, 53, 2022.

[11]Lei Fang, Mark A. Olson, Diego Benítez, Ekaterina Tkatchouk, William A. Goddard III and J. Fraser Stoddart *, "Mechanically bonded," Chem. Soc. Rev.,39, 17-29, 2010.

[12]Ho Yu Au-Yeung * and Yulin Deng, "Distinctive features and challenges in catenane chemistry," Chem. Sci., 13, 3315-3334, 2022.

[13]Qing-Hui Guo, Yang Jiao, Yuanning Feng and J. Fraser Stoddart, "The Rise and Promise of Molecular Nanotopology," Chinese Chemical Society., 3, 7, 1542-1572, 2021.

[14]Guancen Liu, Phillip M. Rauscher, Benjamin W. Rawe, Marissa M. Tranquillia and Stuart J. Rowan, "Polycatenanes: synthesis, characterization, and physical understanding," Chem. Soc. Rev., 51, 4928, 2022.

[15]Phillip M. Rauscher, Kenneth S. Schweizer, Stuart J. Rowan, and Juan J. de Pablo, "Thermodynamics and Structure of Poly-[*n*]-catenane Melts," Macromolecules, 53, 3390−3408, 2020.

[16]Sofia Mena-Hernando and Emilio M. Perez, "Mechanically interlocked materials. Rotaxanes and catenanes beyond the small molecule," Chem. Soc. Rev., 48, 5016, 2019.

[17]S. Pilon, S. Ingemann Jørgensen, J. H. van Maarseveen, "Catenane Synthesis via Covalent Templating," Chem. Eur. J. 27, 2310, 2021.

[18]Gui-Yuan Wu, Hong-Juan Zhu, Fang-Fang Pan, Xiao-Wei Sheng, Ming-Rui Zhang, Xianyi Zhang, Guangxin Yao, Hang Qu and Zhou Lu, "Self-Assembly of [3]Catenane and [4]Catenane Based on Neutral Organometallic Scaffolds," Front. Chem., Volume 9, 2021.

[19]Lydia C. Gilday and Paul D. Beer, "Halogen- and Hydrogen-Bonding Catenanes for Halide-Anion Recognition," Chem. Eur. J. 20, 8379 – 8385, 2014.

[20]Stefano Torresi, Antonino Famulari, and Javier Martí-Rujas, "Kinetically Controlled Fast Crystallization of $M_{12}L_8$ Poly-[*n*]-catenanes Using the 2,4,6-Tris(4-pyridyl)benzene Ligand and $ZnCl_2$ in an Aromatic Environment," J. Am. Chem. Soc., 142, 9537−9543, 2020.

[21]K. Umemoto, K. Yamaguchi, and M. Fujita, "Molecular Paneling via Coordination: Guest-Controlled Assembly of Open Cone and Tetrahedron Structure from Eight Metals and Four Ligands," J. Am. Chem. Soc., 122, 7150-7151, 2000.

[22]D. K. Chand, K. Biradha, and M. Fujita, "Self-Assembly of a Novel Macrocyclic Pd(II) Metallocage Encapsulating a Nitrate Ion," Chem. Commun., 17, 1652-1653, 2001.

[23]M. Fujita, M. Aoyagi, K. Ogura, "Self-Assembly of Macrocyclic Dinuclear Complexes from (en)$Pd(NO_3)_2$ and Pyridine-based Bidentate Ligands," Inorg. Chim. Acta., 246, 53, 1996.

[24]M. Fujita, K. Umemoto, M. Yoshizawa, N. Fujita, T. Kusukawa, and K. Biradha, "Molecular Paneling via Coordination," Chem. Commun., 6, 509-518, 2001.

[25]M. Fujita, Y. J. Kwon, S. Washizu, and K. Ogura, “Preparation, Clathration Ability, and Catalysis of a Two-Dimensional Square Network Material Composed of Cadmium(II) and 4,4'-Bipyridine,” J. Am. Chem. Soc., 116, 1151, 1994.

[26]K. Umemoto, H. Tsukui, T. Kusukawa, K. Biradha, and M. Fujita, “Molecular Paneling by Coordination: An M15L6 Hexahedral Molecular Capsule having Clefts for Reversible Guest Inclusion,” Angew. Chem. Int. Ed., 40, 2620-2622,2001.

[27]Javier Marti-Rujas, Sijie Ma, and Antonino Famulari, “Experimental X‑ray and DFT Structural Analyses of $M_{12}L_8$ Poly‑[n]‑catenanes Using exo-Tridentate Ligands,” Inorg. Chem., 61, 10863−10871, 2022.

[28]Johanna Heine, Jorn Schmedt auf der Gunne, and Stefanie Dehnen, “Formation of a Strandlike Polycatenane of Icosahedral Cages for Reversible One-Dimensional Encapsulation of Guests,” J. Am. Chem. Soc., 133, 10018–10021, 2011.

[29]Shunjie Liu, Yuanyuan Li, Haoke Zhang, Zheng Zhao, Xuefeng Lu, Jacky W. Y. Lam, and Ben Zhong Tang, “Molecular Motion in the Solid State,” ACS Materials Lett., 1, 4, 425–431, 2019.

[30]Marta Morell Cerdà, Burkhard Costisella, Bernhard Lippert, “Synthesis and X-ray crystal structure determination of a useful PdII starting compound, enPd$(NO_3)_2$,” Inorganica Chimica Acta., Volume 359, Issue 5, 1485-1488, 2006.

[31]Y. Yamanoi, Y. Sakamoto, T. Kusukawa, M. Fujita, S. Sakamoto, and K. Yamaguchi, “Dynamic Assembly of Coordination Boxes from (en)Pd(II) Unit and a Rectangular Panel-Like Ligand: NMR, CSI-MS, and X-ray Studies,” J. Am. Chem. Soc.,123,980-981,2001.

[32]WU. QIONG, “Poly-[n]-catenanes: Synthesis of molecular interlocked chains,” SCIENCE., Vol 358, Issue 6369, 1434-143, 2017.

List of Figures

Figure 1.1. Self-assembling process of a MOF.[6] 2
Figure 1.2. Sketch diagram of building block in the synthesis of MOFs.[7] 3
Figure 1.3. Cartoon representation of different types of poly-[*n*]-catenane.[14] 6
Figure 1.4. Catenane formed using the TM method.[14] 7
Figure 1.5. R-CBPQT^{4+} interlock with (DNP38C10).[14].....8
Figure 1.6. $M_{12}L_8$ poly-[*n*]-catenane, the π-π interactions between two benzene ringsmarked as an arrow.[20] 8
Figure 1.7. Cartoon representation of orthogonal pseudorotaxane species, inwhich X is a halogen atom.[19].....8
Figure 1.8. Cartoon representation of the phase transformation.[10].....10
Figure 1.9. Cartoon representation of Pd(II) complex and 4,4'-bipyridine. [24].....12
Figure 1.10. Cartoon representation of the shape of a class of 'rod' ligands.[31].....12
Figure 1.11. Cartoon representation of the shape of a class of triangular.....13
Figure 1.12. Cartoon representation of the process from 1-D to 2-D and 3-D. [24,25].....13
Figure 2.1. Chain of poly-[*n*]-catenanes.[32].....14
Figure 2.2. Structures of TPP; a single cage of $M_{12}L_8$; interlocking $M_{12}L_8$ cages.[28][10] 15
Figure 2.3. Instant synthesis of TPP and $ZnBr_2$ forming 2-o-DCB. [27] 16
Figure 2.4. Powder XRD pattern of the sample(2-o-DCB). [27].....16
Figure 2.5. Comparison between TPB based poly-[*n*]-catenane and white powder(2-o-DCB), a is TPB based poly-[*n*]-catenane, b is white powder(2-o-DCB). [27].....17
Figure 2.6. TG analysis of white powder(2-o-DCB). [27].....17
Figure 2.7. a: PXRD pattern of instant synthesis product of TPP and ZnI_2.....18
Figure 2.8. PXRD pattern of neat grinding products of TPP and ZnI_2 (a), $ZnBr_2$ (b),$ZnCI_2$ (c) PXRD pattern after immersed amorphous product of TPP and ZnI_2 (d),$ZnBr_2$ (e), $ZnCI_2$ (f) into the aromatic templating solvent.[27].....20
Figure 2.9. PXRD of orange powder (top) compared to simulated PXRD from CCDC (bottom). 22
Figure 2.10. Cartoon representation of molecular panel of 4,4'-bipyridine ligand.....23
Figure 2.11. Structure prediction of 4,4'-bipyridine and enPd$(NO_3)_2$ as reported by Fujita. [25] ..23

Figure 2.12. Structure of the square complex self-assembled using 4,4'-bipyridine and enPd(NO_3) 24
Figure 2.13. Molecular panel of TPT and TPB. 25
Figure 2.14. The M_6L_4 cage formed by TPT and enPd(NO_3)$_2$.[24] 25
Figure 2.15. Aromatic range ^{1}H NMR spectra of samples taken at different reaction time (5mins, 15mins, 25mins, 40mins, 50mins). 27
Figure 2.16. Aromatic range ^{1}H NMR spectra zoom in of samples taken at reaction time 50 mins. 28
Figure 2.17. Non-aromatic range ^{1}H NMR spectra of samples taken at differentreaction times (5mins, 15mins, 25mins, 40mins, 50mins). 29

Ringraziamenti

A long time has passed since I entered Politecnico di Milano. A lot has been experienced in recent years, including but not limited to exams, independent living, city lock down and unfamiliar environments. It's time to sum up and express gratitude.

First of all, I would like to thank Professor Javier Martí-Rujas, who gives me the opportunity to explore the field of coordination chemistry, patiently guiding me allowed me to grow from a state of ignorance to a certain understanding of this field. Especially in the writing of the graduation thesis, not only provide language modification, but also take the trouble to correct theoretical errors and interpret. It's lucky to meet Professor Javier.

Stefano Elli is a friendly, helpful and professional colleague. He knows a lot of things, not only guides me in the experiment, but also gives me advice and help with exams. I wish him to enjoy his PhD research and achieve satisfactory results. Besides, the other colleagues in the lab were also warm and friendly.

My family supports me for a long time, without their moral and financial support, I would not have been able to get through these meaningful three years in Milano, Italy.

Finally, my grandparents, two elderly people are my greatest spiritual sustenance and motivation. My grandmother, in particular, hopes that she can tenaciously overcome cancer at the age of eighty-three. This will be my greatest wish.